

# Progress on the Development of Lightweight Dual Frequency/Polarized Microstrip Antenna Arrays on Liquid Crystal Polymer (LCP) Substrates for Remote Sensing of Precipitation

Gerald DeJean<sup>1</sup>, Dane Thompson<sup>1</sup>, Guoan Wang<sup>1</sup>, Ramanan Bairavasubramanian<sup>1</sup>, RongLin Li<sup>1</sup>, George E. Ponchak<sup>2</sup>,  
Manos Tentzeris<sup>1</sup> and John Papapolymerou<sup>1</sup>

<sup>1</sup>School of Electrical and Computer Engineering, Georgia Institute of Technology, Atlanta, GA 30332-0250

<sup>2</sup>NASA Glenn Research Center, Cleveland, OH, 20032

**Abstract-** This paper presents the most recent results towards the development of a lightweight dual frequency/polarization microstrip antenna array on Liquid Crystal Polymer (LCP) substrates for NASA's remote sensing applications. LCP's multi-layer lamination capabilities, excellent electrical and mechanical properties, and near hermetic nature make it an excellent candidate for the development of low cost, flexible antenna arrays with integrated RF MEMS switches for NASA's applications up to 110 GHz. To test the viability of LCP at these frequencies, ring resonators and cavity resonators have been used to characterize LCP's  $\epsilon_r$  and  $\tan\delta$  from 2 – 110 GHz for the first time. Dual-frequency antenna arrays at 14 and 35 GHz were developed. Also, a soft-and-hard surface (SHS) structure has been employed for radiation pattern improvement of a patch antenna on a large-size substrate.

## I. INTRODUCTION

It is the NASA Earth Science Enterprise's (ESE) goal to develop a scientific understanding of the Earth's environmental system and its response to natural and man-made changes, which will enable better prediction of climate, weather, and natural hazards. This will lead to expanded and accelerated realization of economic and societal benefits. However, to achieve these goals, NASA and the scientific community needs to develop and adopt advanced technologies to accurately monitor and measure the global precipitation, evaporation, and cycling of water. To monitor precipitation patterns, NASA requires dual-frequency (14/35 GHz for rain and 19/37 GHz for snow), dual-polarization radar and radiometers. The common requirement in these radars is the need for low-cost, low mass, deployable antennas with large surface area that can be rolled-up or folded for launch and then deployed in space. In addition, electronic scanning and shaping of the radiation patterns at the different frequencies is also desirable. For this purpose, we plan to develop a prototype 2x2 dual frequency/polarization microstrip antenna array on an organic substrate (liquid crystal polymer) with integrated RF MEMS phase shifters operating at 14/35 GHz.

LCP is a material whose mechanical strength, adhesion to copper, and via drilling/metallization have all recently been optimized to enable its use in microwave circuit construction [1-2]. A unique extrusion process, surface treatments, and experiments with laser, chemical, and reactive ion etch (RIE) gases have been used to overcome its previous process limitations [3-4]. LCP is nearly hermetic, has very good electrical properties ( $\epsilon_r = 2.9-3.0$ ,  $\tan \delta = 0.002-0.003$ ), is recyclable, has a wide range of CTE (0-30 ppm/°C), has

excellent chemical resistance, is flexible, and it is capable of multilayer lamination. For multilayer LCP circuits, a 1 mil low melting temperature (290°C) LCP layer can be used to bond high melting temperature (315°C) LCP core layers which typically come in 2 – 8 mil thicknesses. Electrical properties of the two types are the same. Thus, compact, vertically integrated architectures performing as the substrate and package may be realized in LCP material. And the cost of LCP (~\$5/ft<sup>2</sup>) [5], though not yet competitive with FR-4, is already reasonable and should continue to drop as production levels grow.

In this paper we focus on simulated and measured results from a prototype 2x1 dual-frequency antenna array at 14 and 35 GHz. In addition, simulations of a radiation pattern improving SHS structure, measured results for an RF MEMS switch on LCP, and LCP loss tangent/dielectric constant characterization from 30-110 GHz are presented.

## II. ARRAY DESIGN AND SIMULATED AND MEASURED RESULTS

The architecture of the dual-polarization, single frequency microstrip antenna array at 14 and 35 GHz is shown in Fig. 1. The total thickness of the LCP substrate is 425  $\mu\text{m}$ . The metals, used in simulation and fabrication, for the ground plane and the antenna elements were copper (Cu) and had a thickness of 18  $\mu\text{m}$ . The total substrate thickness (h) for the design was 425  $\mu\text{m}$ , consisting of two LCP layers (each 200  $\mu\text{m}$  thick) and a 25  $\mu\text{m}$  bonding layer. The 35 GHz antenna array was placed on the top surface of the LCP substrate (at the interface of LCP and air), while the 14 GHz antenna array was embedded on a 200  $\mu\text{m}$  layer ( $h_1$ ) for compactness and to minimize crosstalk. Two distinct design approaches are considered: a symmetrically-fed array at 14 and 35 GHz and an asymmetrically-fed array at the same two frequencies. The schematic is shown in Fig. 2. The purpose of proposing two different approaches is to investigate the variation in the designs with respect to their performance. The four arrays are designed independently and then fine tuned before integration in order to optimize the impedance matching and radiation characteristics across both the bands. The feed network for each band is placed in the same layer as the corresponding radiating element, again in order to minimize the cross coupling and improve isolation between the two arrays. Moreover, this approach avoids the need for any vertical connection (vias) thereby simplifying the fabrication process. Careful consideration must be taken in order to minimize the crosstalk between the feed network and the radiating element since both of them are placed in the same layer. The control of polarizations was realized by the use of two small gaps in the feedlines for two perpendicular directions, which introduced a small capacitance in each gap. The small capacitance on the

order of fF's in the gap represents high impedance or a “near” electrical open circuit which prevents the mode excitation of the corresponding polarization. To avoid parasitic coupling between the two arrays, the asymmetric array at 35 GHz has a cross configuration, which in reality is a square configuration that is rotated by 45 degrees with respect to the shape of the 14 GHz array. Since this 2x2 array employs only canonical shapes, it can be fabricated in a quite straightforward way and easily cascaded in both longitudinal and transverse directions. Preliminary theoretical derivations show that 24 arrays of this type could provide a beamwidth smaller than 2 degrees. Furthermore, the LCP substrate allows for the integration of RF MEMS switches for polarization diversity capabilities.

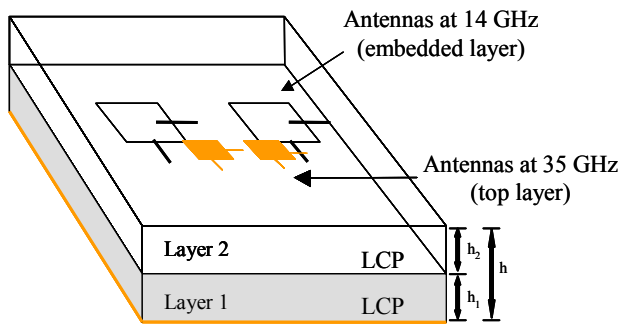


**Figure 1.** The proposed 2x1 dual frequency/polarization patch antenna array architecture on multilayer LCP substrate.

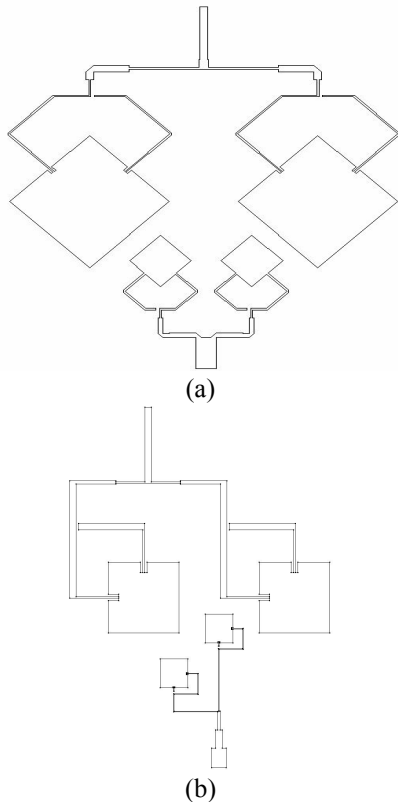
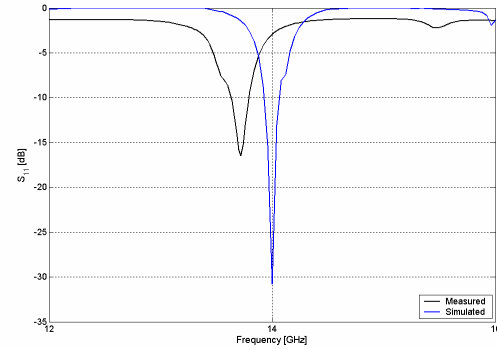


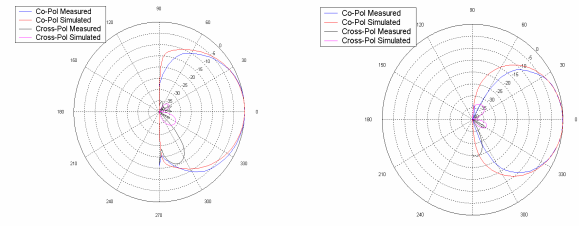
**Figure 2.** Schematic of the simulated 2x1 design for: a) symmetrically-fed array and b) asymmetrically-fed array.

The two arrays were simulated using two full-wave simulators: EmPicasso and Microstripes 6.0. EmPicasso

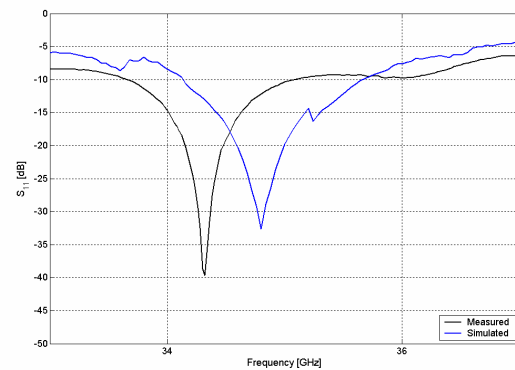
assumes an infinite ground size while MicroStripes allows finite ground size to be realized so that backside radiation and edge diffraction effects can be accounted for in the simulation. Measurements were also taken for the fabricated 2x1 arrays. The array was mounted on an aluminum fixture that included a coaxial-to-microstrip connector to facilitate the s-parameter measurement. An SOLT calibration was performed with the reference planes at the end of the coaxial cables. Figs. 3 and 4 show the return loss and 2D radiation pattern results obtained from the simulated and the measured symmetrically-fed and asymmetrically-fed arrays, respectively. The single frequency array is excited while the other array is acting as a parasitic element.



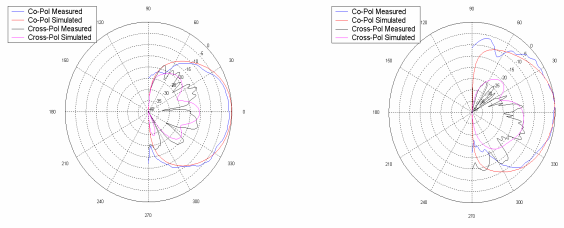
(a)



(b)

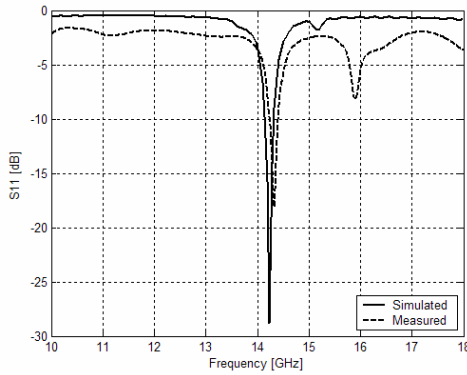


(c)

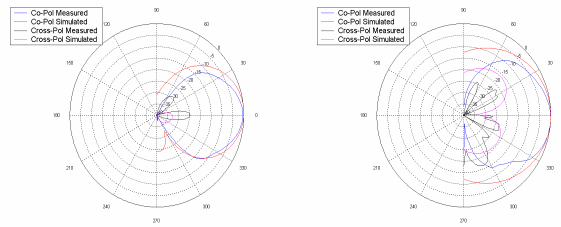


(d)

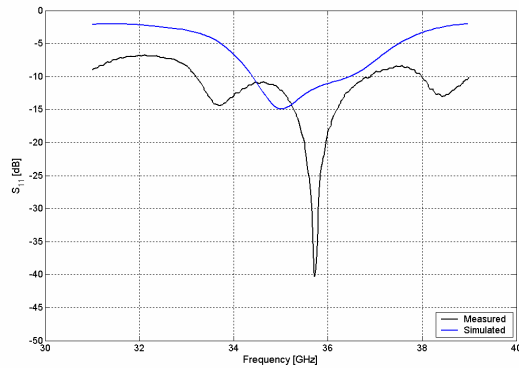
**Figure 3.** Simulated and measured results for the 2x1 symmetrically-fed array (one polarization): a) return loss at 14 GHz, b) radiation patterns at 14 GHz, c) return loss at 35 GHz, and d) radiation patterns at 35 GHz.



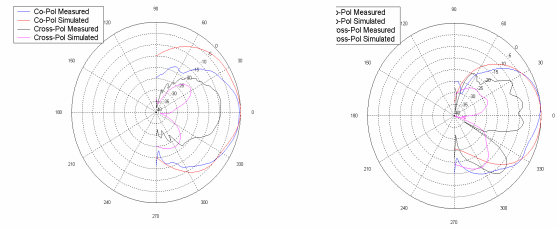
(a)



(b)



(c)



(d)

**Figure 4.** Simulated and measured results for the 2x1 asymmetrically-fed array (one polarization): a) return loss at 14 GHz, b) radiation patterns at 14 GHz, c) return loss at 35 GHz, and d) radiation patterns at 35 GHz.

It can be seen that very good agreement is observed between the simulated and measured results for the return loss and radiation patterns. It is worth noting that the impedance bandwidth of the measured asymmetrically-fed array at 35 GHz is twice as wide as expected due to the existence of parasitic effects. These parasitic effects can be attributed to connector and cable losses in the measurement process. The two configurations exhibited a return loss of better than 15 dB, while the measured beamwidths are consistent with the simulated results.

### III. RADIATION PATTERN IMPROVEMENT WITH SOFT-AND-HARD SURFACES (SHS)

When a patch antenna is fabricated on a larger-size substrate, its radiation pattern may be considerably affected by the diffraction of surface waves at the edge of the finite grounded substrate [6]. The most popular technique for the improvement of the radiation performance of patch antennas on a large-size substrate is to construct an artificial periodic structure, such as photonic bandgap (PBG) or electromagnetic bandgap (EBG) [7], surrounding the patch antenna to prevent the surface waves from propagating in the substrate. Unfortunately, it requires a considerable area to form a complete band gap structure. Therefore, the concept of the modern SHS structure is applied to improve the radiation pattern of patch antennas. The effectiveness of the compact SHS structure in terms of radiation pattern improvement is verified by its implementation on LTCC multilayer technology.

Consider a probe-fed square patch antenna on a square grounded substrate with thickness  $H$  and a dielectric constant  $\epsilon_r$ . The patch antenna is surrounded by a square compact SHS structure, as shown in Fig. 5. The substrate thickness has a lateral size of  $L \times L$ , much larger than the size the square patch ( $L_p \times L_p$ ). The ideal compact SHS structure consists of a square ring of metal strips that are short-circuited to the ground plane by a metal wall along the outer edge of the ring. The inner length of the SHS ring (denoted by  $L_s$ ) was found to be approximately one wavelength plus  $L_p$ . The width of the metal strip ( $W_s$ ) is approximately equal to a quarter of the guided wavelength.

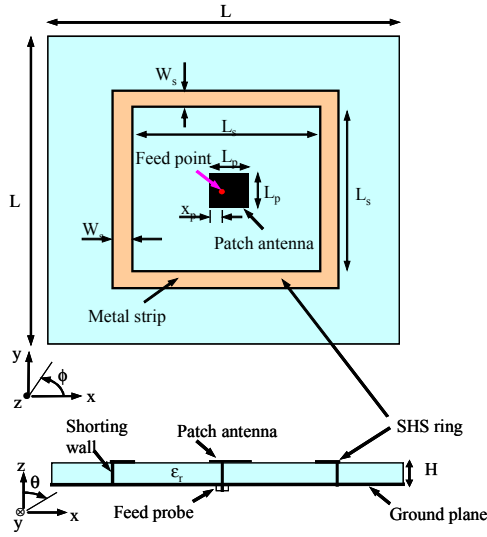


**Figure 5.** Patch antenna surrounded by an ideal compact SHS structure.

The simulated 3D radiation patterns of the stacked-patch antennas with and without the SHS are shown in Fig. 6. It is observed that there is a deep drop in the z-direction for the antenna without SHS due to the diffraction of surface waves at the edge of the substrate. The degradation of radiation pattern is significantly improved by the via-incorporated SHS. The design frequency was 16.5 GHz. The SHS can also be applied to LCP multilayer substrates.

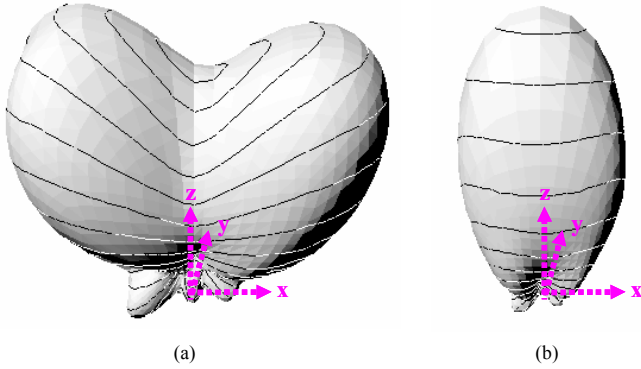


**Figure 6.** 3D radiation patterns of the patch antennas: a) without SHS and b) with the SHS.

#### IV. MEMS SWITCH ON LCP

To fabricate the MEMS switch on an LCP substrate, a simple four mask process is used as shown in Fig. 7. A 3  $\mu\text{m}$  PI2610 polyimide is first spun on LCP to planarize the surface and minimize the roughness. The CPW signal lines then were fabricated by evaporating Ti/Au/Ti (300Å/5000Å/300Å). PECVD  $\text{Si}_3\text{N}_4$  layer was patterned between the membrane and the signal line. A 1.8 $\mu\text{m}$  thick photoresist (1813) was spin coated and patterned to create the air-gap. Ti/Au/Ti (300Å/3000 Å/300 Å) seed layer was then evaporated and patterned and electroplated. Finally, after removing the sacrificial photoresist layer with a resist stripper, a critical point drying process was used to release the switches.

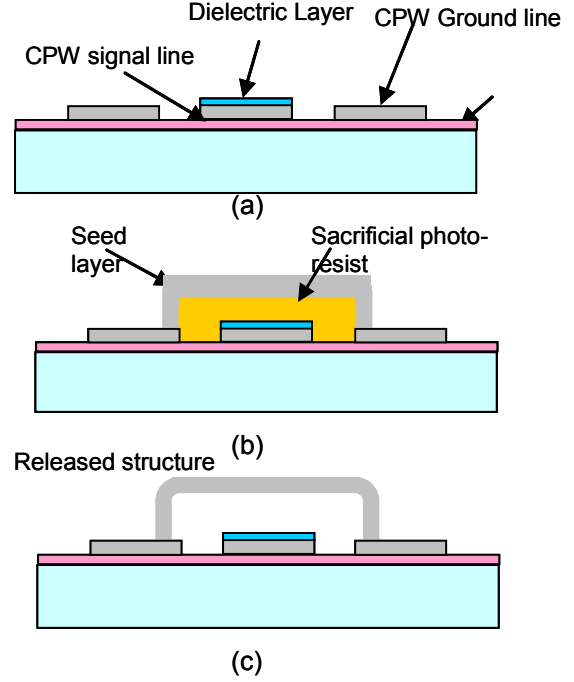


**Figure 7:** Fabrication process flow of switch.

A Scanning Electron Microscope (SEM) picture of the fabricated air-bridge type CPW switch structure with a 1.2 $\mu\text{m}$  thick gold membrane, a 1.8 $\mu\text{m}$  air-gap and a membrane size of 100x200  $\mu\text{m}^2$  is shown in Fig. 8.

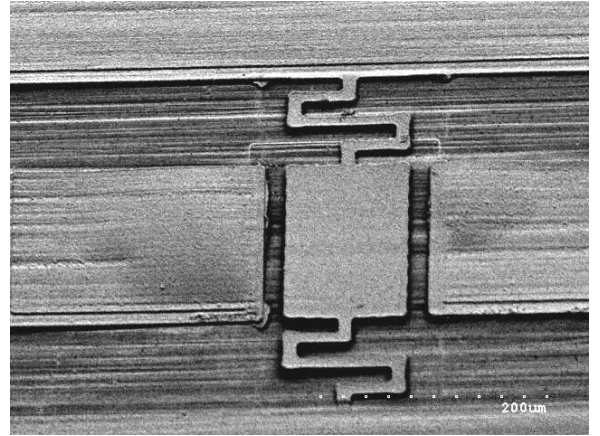


**Figure 8.** SEM of a fabricated air-bridge type CPW switch on LCP with 1.2 $\mu\text{m}$  thick Au membrane and meander-shaped support

#### V. MEASURED RESULTS OF MEMS SWITCH ON LCP

Measurements of the air-bridge type switch were taken using an Agilent 8510 network analyzer. A TRL calibration was performed to de-embed the coplanar line and transition losses. Measured results for the nitride switches with silicon substrate and LCP are shown in Figs. 9-10. The pull-down voltage was measured to be 25 V. For the LCP switch, when

the switch is activated, the isolation is around 20 dB at 20 GHz and  $C_{ON}=3$  pF, while the return loss is around 0.1 dB at 20 GHz. When the switch is in the UP position, the insertion loss is around 0.08 dB at 20 GHz and  $C_{OFF}=35$  fF, the return loss is 18 dB at 20 GHz. For the same switch on silicon substrate, when the switch is activated, the isolation is around 17 dB at 20 GHz and  $C_{ON}=2$  pF, while the return loss is around 0.4 dB at 20 GHz. When the switch is in the UP position, the insertion loss is around 0.8 dB at 20 GHz and  $C_{OFF}=25$  fF, the return loss is 10 dB at 20 GHz. The deteriorated return loss of switch on silicon is due to the thinner sacrificial layer that increases the capacitance, while the different  $C_{ON}$  between the two types of switches with different substrate is because the thickness of Silicon nitride is a little different. All air-bridge switches with LCP substrate have better insertion loss than that of the switches with silicon substrate at down state, and at up state, all the LCP switches have smaller insertion loss is due to extreme lower dielectric loss tangent of LCP substrate.

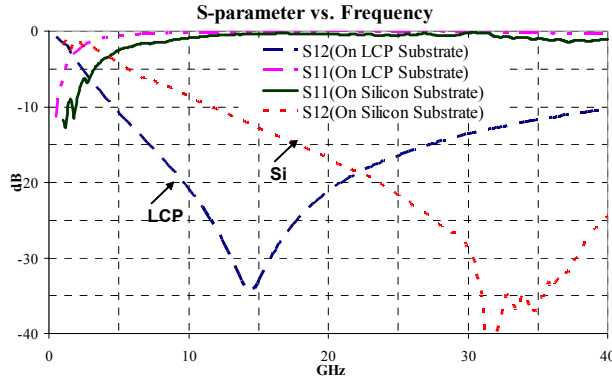


**Figure 9:** Measured S-parameters for the Air-bridge switch with Silicon and LCP substrate in DOWN state.

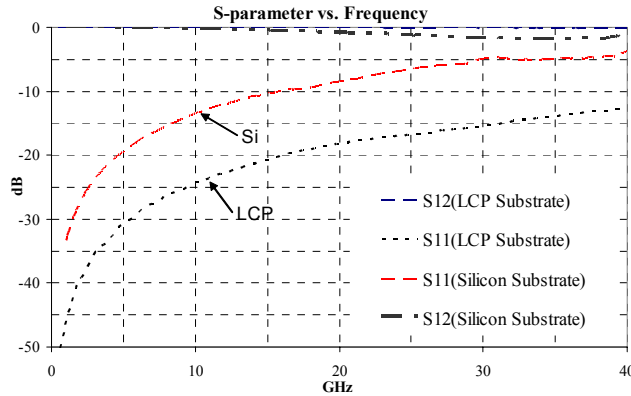


**Figure 10:** Measured S-parameters for the air-bridge switch with Silicon and LCP substrate in UP state

## VI. MILLIMETER-WAVE LCP LOSS TANGENT AND DIELECTRIC CONSTANT CHARACTERIZATION

Two complementary methods were used to extract LCP's dielectric constant and loss tangent from 30-110 GHz. Previous characterization was reported only below 35 GHz [8-10]. The first method utilized microstrip ring resonators and the second involved cavity and split-post cavity resonators. A

description of this characterization process may be found in [11]. The results are shown in Figs. 11-12.

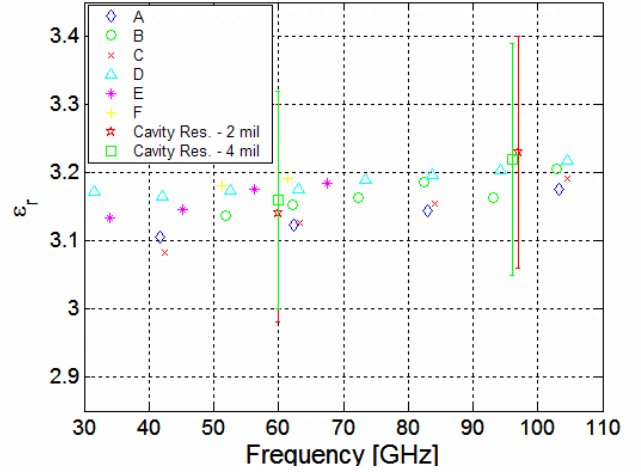


**Figure 11:** LCP's measured dielectric constant with ring resonator designs A-F and cavity resonators near 60 and 97 GHz.

The dielectric constant of LCP is seen to have a minor frequency dependence, rising slightly with increasing frequency. The approximate dielectric constant is summarized in (1).

$$\epsilon_r = 3.16 \pm 0.05 \text{ for } (30 \text{ GHz} < f < 110 \text{ GHz}) \quad (1)$$

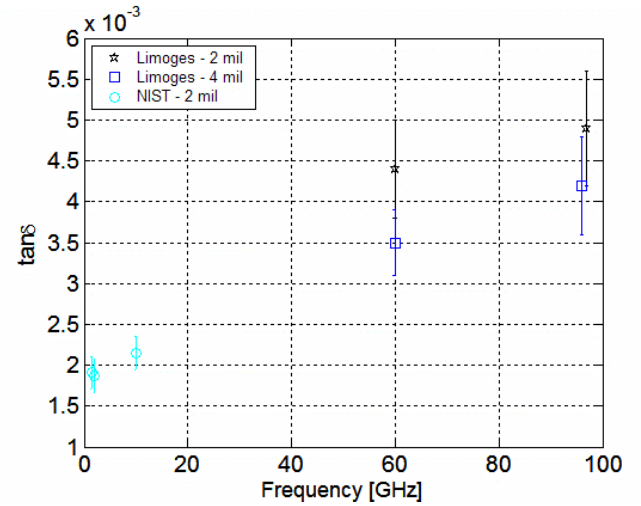


**Figure 12:** LCP's measured loss tangent with cavity resonators near 60 and 97 GHz.

LCP's loss tangent also appears to increase with increasing frequency, though it remains low even at 97 GHz. An accurate linear approximation that matches measurements from 2-97 GHz is given in (2).

$$\tan\delta(f) = 2.6437 \cdot 10^{-5} \cdot (f[\text{GHz}]) + 0.0019 \quad (2)$$

## V. CONCLUSIONS

This paper presented the most recent results towards the development of a low cost, flexible and low-loss dual frequency/polarization patch antenna array on LCP substrate for the 14/35 GHz precipitation radar. Measured return loss for the antennas is greater than 15 dB and the radiation patterns are consistent with simulations. Furthermore, an SHS structure was used to improve the shape of the radiation pattern of an antenna on a large-size substrate. An RF MEMS switch on LCP shows a very good RF performance with the potential of making integrated MEMS phase shifters on LCP. Finally, promising broadband electrical properties for LCP have been found by measuring its dielectric constant and loss tangent for the first time from 30-110GHz.

## ACKNOWLEDGMENTS

This work was supported by NASA under contract #NCC3-1015. The authors would also like to extend a special thanks to the following people and/or organizations for their help with the fabrication:

Georgia Electronic Design Center  
Cliff Roseen and Colleen Murphy, Rogers Corporation  
Georgia Tech Microelectronics Research Center  
Georgia Tech Packaging Research Center

## REFERENCES

- [1] *PMTEC LCP Materials Symposium*, Huntsville, AL, October 29, 2002. unpublished.
- [2] T. Suga, A. Takahashi, M. Howlander, K. Saijo, and S. Oosawa, "A lamination technique of LCP/Cu for electronic packaging," *2<sup>nd</sup> Intl. IEEE Conference on Polymers and Adhesives in Microelectronics and Photonics*, pp. 177-182, June 2002.
- [3] T. Zhang, W. Johnson, B. Farrell, and M. St. Lawrence, "The processing and assembly of liquid crystalline polymer printed circuits," *2002 Int. Symp. on Microelectronics*, 2002.
- [4] X. Wang, L. Lu, and C. Liu, "Micromachining techniques for liquid crystal polymer," *14<sup>th</sup> IEEE Intl. Conf. on MEMS*, pp. 21-25, January 2001.
- [5] C. Murphy, Rogers Corporation, private communication, January 2004.
- [6] S. Maci, L. Borelli, and L. Rossi, "Diffraction at the edge of a truncated grounded dielectric slab," *IEEE Trans. Antennas Propagat.*, vol. 44, pp. 863-872, June 1996.
- [7] R. Gonzalo, P. de. Maagt, and M. Sorolla, "Enhanced patch-antenna performance by suppressing surface waves using photonic-bandgap substrates," *IEEE Trans. Microwave Theory Tech.*, vol. 47, no. 11, pp. 2131-2138, Nov. 1999.
- [8] K. Jayaraj, T. E. Noll, and D. R. Singh, "RF characterization of a low cost multichip packaging technology for monolithic microwave and Millimeter Wave Integrated Circuits," *URSI Intl. Symp. on Signals, Systems, and Electronics*, pp. 443-446, October 1995.
- [9] G. Zou, H. Gronqvist, P. Starski, and J. Liu, "High frequency characteristics of liquid crystal polymer for system in a package application," *IEEE 8<sup>th</sup> Intl. Symp. on Adv. Packag. Materials*, pp. 337-341, March, 2002.
- [10] G. Zou, H. Gronqvist, J. Piotr Starski, and J. Liu, "Characterization of liquid crystal polymer for high frequency system-in-a-package applications," *IEEE Trans. Adv. Packag.*, vol. 25, No. 4, November 2002.
- [11] D.C. Thompson, O. Tantot, H. Jallageas, G.E. Ponchak, M.M. Tentzeris, and J. Papapolymerou, "Characterization of Liquid Crystal Polymer (LCP) Material and Transmission Lines on LCP Substrates from 30-110 GHz", *IEEE Trans. Microwave Theory Tech.*, Vol.52, No.4, pp.1343-1352, April 2004.